



Published in final edited form as:

Mol Cell. 2013 June 6; 50(5): 749–761. doi:10.1016/j.molcel.2013.04.007.

A transcriptome-wide RNAi screen in the *Drosophila* ovary reveals novel factors of the germline piRNA pathway

Benjamin Czech^{1,#,2}, Jonathan B. Preall^{1,2}, Jon McGinn¹, and Gregory J. Hannon^{1,#}

¹Watson School of Biological Sciences, Howard Hughes Medical Institute, Cold Spring Harbor Laboratory, Cold Spring Harbor, New York 11724, USA

Summary

The *Drosophila* piRNA pathway provides an RNA-based immune system that defends the germline genome against selfish genetic elements. Two inter-related branches of the piRNA system exist: somatic cells that support oogenesis only employ Piwi, whereas germ cells utilize a more elaborated pathway centered on the three gonad-specific Argonaute proteins Piwi, Aubergine, and Argonaute3. While several key factors of each branch have been identified, our current knowledge is insufficient to explain the complex workings of the piRNA machinery. Here, we report a reverse genetic screen spanning the ovarian transcriptome in an attempt to uncover the full repertoire of genes required for piRNA-mediated transposon silencing in the female germline. Our screen reveals new key factors of piRNA-mediated transposon silencing, including the novel piRNA biogenesis factors, *CG2183* (*GASZ*) and *Deadlock*. Last, our data uncovers a previously unanticipated set of factors preferentially required for repression of different transposons types.

Keywords

Drosophila; RNAi; piRNA pathway; transposon silencing; germ cells

Introduction

Eukaryotic organisms of all phyla are constantly challenged by a myriad of genomic parasites (Malone and Hannon, 2009; Siomi et al., 2011). These mobile elements are broadly classified based on their transposition strategy. Retrotransposons employ an RNA intermediate during mobilization, whereas DNA transposons directly excise and insert their genomic information into new locations (Slotkin and Martienssen, 2007). While expression patterns for elements of both classes vary widely over a range of spatial and temporal niches, the reproductive system invariably suffers the majority of transposable element activity in the host organism. Alterations to the host genome caused by transposition, such as disruptions to coding or regulatory regions, double-strand breaks, or chromosomal rearrangements, are generally deleterious and reduce reproductive fitness when they occur in

© 2013 Elsevier Inc. All rights reserved.

[#]Correspondence: czech@cshl.edu or hannon@cshl.edu.

²contributed equally

Accession Numbers

RNAseq and small RNA data were deposited in the Gene Expression Omnibus database under accession number GSExxxxx (pending).

Publisher's Disclaimer: This is a PDF file of an unedited manuscript that has been accepted for publication. As a service to our customers we are providing this early version of the manuscript. The manuscript will undergo copyediting, typesetting, and review of the resulting proof before it is published in its final citable form. Please note that during the production process errors may be discovered which could affect the content, and all legal disclaimers that apply to the journal pertain.

the germ cell lineage (Khurana and Theurkauf, 2010; Malone and Hannon, 2009; Senti and Brennecke, 2010; Siomi et al., 2011).

Small RNAs play a central role in transposon control in eukaryotes. Efficient suppression of mobile elements in animal germ cells relies on the conserved piRNA pathway, whose core is composed of Argonaute proteins of the PIWI-clade and their 23- to 28-nt small RNA partners known as piRNAs (Khurana and Theurkauf, 2010; Malone and Hannon, 2009; Senti and Brennecke, 2010; Siomi et al., 2011). To a rough approximation, the piRNA pathway can be seen as RNA-based immune system with innate and adaptive components to its defensive response (Brennecke et al., 2007). The targets of the primary piRNA pathway are genetically hardwired in the form of piRNA clusters, which contain transposon remnants that serve as witness to prior exposure to mobile elements (Aravin et al., 2006; Brennecke et al., 2007; Girard et al., 2006). Additionally, an adaptive amplification mechanism known as the ping-pong cycle attunes the intensity of the piRNA response by feeding back sequence information from the active elements themselves to generate and amplify silencing triggers (Brennecke et al., 2007; Gunawardane et al., 2007; Li et al., 2009; Malone et al., 2009).

The piRNA pathway is probably best understood in the ovary of *Drosophila melanogaster*, which comprises two gonadal tissue types each deploying its own unique piRNA system (Malone et al., 2009). The germline is composed of the transcriptionally inactive oocyte and the syncytial nurse cells, which express all three *Drosophila* PIWI-clade proteins, *P*-element induced wimpy testis (Piwi), Aubergine (Aub), and Argonaute3 (AGO3). Germ cells generate piRNAs derived from specific piRNA clusters as well as from active transposable elements via the ping-pong cycle (Brennecke et al., 2007; Gunawardane et al., 2007; Li et al., 2009; Malone et al., 2009). In contrast, the somatic cell lineage that surrounds and supports the germline only expresses Piwi, transcribes piRNAs derived from separate, soma-specific clusters, and does not engage in ping-pong amplification (Brennecke et al., 2007; Lau et al., 2009; Malone et al., 2009; Saito et al., 2009). The varying expression and sub-cellular localization patterns of the PIWI-family proteins reflect differences in the biogenesis of the piRNAs that fuel them as well as the molecular modes of silencing they employ.

Primary piRNA biogenesis appears to follow similar routes in somatic and germline cells and is initiated with transcription of precursors from lineage-specific piRNA clusters. Processing of cluster transcripts is thought to take place after export to the cytoplasm, likely at specialized perinuclear foci marked by known components of the piRNA biogenesis machinery. Current models suggest that cluster transcripts are parsed linearly into multiple intermediates that feature the 5' end of the mature piRNA but are extended at their 3' end. Following loading into Piwi (and in the germline, Aub), which takes place at in perinuclear structures called Yb-bodies in the soma and nuage in the germline (Handler et al., 2011; Olivieri et al., 2010; Qi et al., 2011; Saito et al., 2010; Szakmary et al., 2009), the bound piRNA is matured through 3' trimming by a yet-to-be identified exonuclease (Kawaoka et al., 2011). Mature Piwi-RISC enters the nucleus to silence complementary transposons by transcriptional gene silencing via triggering of repressive chromatin marks (Le Thomas et al., 2013; Rozhkov et al., 2013; Sienski et al., 2012).

The ping-pong amplification loop, in contrast, only operates in germline cells and serves to detect and post-transcriptionally silence highly active transposon threats. Input for the ping-pong cycle is received either from primary biogenesis of cluster transcripts or from maternally deposited piRNAs associated with Aub (Brennecke et al., 2008; Malone et al., 2009). PiRNAs in an antisense orientation to transposons guide Aub to appropriate mRNA substrates, leading to target cleavage. The resulting cleavage product loads into AGO3, and following exonucleolytic trimming and methylation yields mature AGO3-RISC associated with sense piRNAs. These transposon-derived piRISCs complete the ping-pong cycle by

pairing with and cleaving more cluster transcripts to produce further Aub-loaded antisense piRNAs (Brennecke et al., 2007; Gunawardane et al., 2007). Numerous factors have been linked to the ping-pong cycle, with most of them localizing to nuage and a prominent subset being members of the Tudor protein family (Anand and Kai, 2012; Handler et al., 2011; Lim and Kai, 2007; Malone et al., 2009; Patil and Kai, 2010; Zamparini et al., 2011; Zhang et al., 2011).

The vast majority of currently known piRNA pathway components were originally identified by forward genetic approaches in classical screens aimed to uncover mutations that affect oogenesis, female fertility or spindle formation (Schupbach and Wieschaus, 1989, 1991) and were only linked to the piRNA pathway later. Although reverse genetics utilizing transgenic RNAi have proven powerful to reveal novel factors in many studied pathways in somatic tissues, technical limitations prevented the application of RNAi in the female germline until recently. However, through overexpression of Dcr2, we and others have recently demonstrated the effectiveness of transgenic RNAi in germ cells of the female ovary (Handler et al., 2011; Preall et al., 2012; Wang and Elgin, 2011), enabling us to apply this technology to uncover missing piRNA pathway components on a large scale.

Although we are beginning to understand basic concepts of piRNA-mediated silencing, many important aspects of the pathway are still enigmatic due to gaps in our knowledge of central factors such as nucleases and silencing effectors. Thus, we designed an RNAi-based screen to systematically probe for missing components of the piRNA system *in vivo*. To cover the broadest range of new factors, we specifically targeted the germline pathway, which comprises both primary biogenesis and the ping-pong cycle (Malone et al., 2009). Here, we report the results of this screen, which spans the ovarian transcriptome, with the discovery of 74 genes (including already known piRNA pathway components), whose knockdown caused strong de-repression of one or more of four individual transposons. Secondary assays enabled us to distinguish factors involved in the production of primary and/or secondary piRNAs from those required for silencing effector steps carried out by Piwi or Aub/AGO3 complexes.

Results

Screening assays to monitor transposon de-repression

In order to limit the number of labor-intensive crosses to be performed, we first cataloged the observable ovarian transcriptome of our screening stock that carries a *Dcr2* transgene and the *nos*-GAL4 driver by RNAseq. We found significant expression levels for 8,396 protein-coding genes (average FPKM > 1) (Figure 1A, top), which corresponds to 60.86% of *Drosophila melanogaster* genes. As the ovary consists of both somatic and germline tissue, we compared our ovarian RNAseq data with experiments carried out on RNA from Ovarian Somatic Sheet (OSS) cells (Niki et al., 2006), early embryos (indicator for germline RNAs as only those are deposited), and ovariectomized carcasses with the goal to identify germline-enriched genes. In general, we found strong correlations between entire ovaries and the other two ovary-related data sets (embryo: $R^2 = 0.457$; OSS: $R^2 = 0.603$), with little correlation of expression levels in data sets derived from ovaries and carcasses ($R^2 = 0.151$) (Figure S1A). The high correlation between the ovarian transcriptome and RNAseq from embryos and OSS is also evident by the pronounced overlap of expressed genes with FPKM > 1 (Figure S1B). Comparing datasets, we see no genes that are significantly ($P < 0.01$) expressed at FPKM < 1 in ovary versus carcass, suggesting that we are unlikely to miss any ovary-specific genes by selecting this value as cutoff for screening (Figure S1C). We conclude that our transcriptome analysis identified ovarian-expressed genes with sufficient stringency to serve as a filter for selecting screening targets.

Of the 8,396 genes expressed in ovaries, 8,171 (97.3%) were covered by RNAi lines in the Vienna *Drosophila* RNAi Center (VDRC) collection (Figure 1A, bottom) (Dietzl et al., 2007). To deplete factors specifically in germ cells, we used our previously reported knockdown strategy: males carrying the UAS-driven dsRNA were crossed to virgin females containing the germline-specific driver *nos*-GAL4 and a UAS-*Dcr2* transgene, which was previously shown to increase knockdown efficiency (Handler et al., 2011; Preall et al., 2012; Wang and Elgin, 2011). Applying this strategy to deplete *Armi* and *Spn-E* from germ cells resulted in dramatic and selective de-repression of germline-dominant transposons using two independent dsRNA lines, similar to earlier results (Preall et al., 2012), while knockdown of the soma-specific component *Yb* had no effect on transposon levels (Figure 1B) (Handler et al., 2011; Olivieri et al., 2010; Qi et al., 2011; Saito et al., 2010). Due to their consistent and robust fold increases compared to *white* (*w*) knockdowns, we based our screen on two LINE-like elements *HeTA* and *TAHRE*, as well as the LTR elements *burdock* and *blood*. For these preliminary measurements, we used RNA isolated from dissected ovaries and standard SYBR green-based qPCR assays.

To achieve the throughput necessary for a large-scale screen, we isolated RNA in 96-well format from whole adult females. Combination of this strategy with optimized, sensitive *TaqMan* qPCR assays provided comparable sensitivity and dynamic range to dissected ovaries, making it an ideal screening platform (Figure 1C). Furthermore, we confirmed the specificity of our system by germline knockdown of the soma-specific component *Yb*, which caused no significant change in transposon levels. We further optimized our workflow by using *TaqMan* assays that allowed multiplexed qPCRs with the normalization standard *rp49* and the probed transposons in the same reaction tube.

To identify piRNA pathway components required for transposon silencing, we setup trays containing 96 crosses, each containing *w* and *armi* control knockdowns. Flies were allowed to mate for 7 days and then discarded. Offspring flies were transferred to fresh food vials 5 days later and allowed to mature for 2.5 additional days. Of each cross, we transferred six females into 96-well collection tubes, and performed RNA isolation, reverse transcription and multiplexed qPCR. Data was analyzed and *z*-scores were calculated for each plate (Figure 1D).

Comprehensive identification of factors required for proper transposon silencing

We screened a collection of 8,171 dsRNA lines *in vivo* for genes involved in piRNA silencing for four individual transposons (see Table S1 for list of screened genes and their transposon expression). To increase the stringency for potential candidates, we also calculated the average of the four individual transposon *z*-scores and computed heat maps for average and individual transposon data (Figure 2A). Requiring an average *z*-score of -1.5 or lower, our primary screen only identified 216 out of all 8,171 probed dsRNA lines (2.64%) to result in robust transposon de-repression. Strikingly, using this threshold for candidate selection, all of the positive *armi* controls were included, whereas none of the negative *w* controls was (Figure 2C), with similar results obtained when transposons were assessed individually (Figure S2). Based on the magnitude of transposon de-repression, we further categorized these candidates into “weak” and “strong”, with knockdown of 74 genes that resulted in average *z*-scores of -2 or lower in the “strong” class (Figure 2B). Using these more stringent criteria, we found all known piRNA pathway components (except *Egg*), thus providing internal validation for our screen.

Validation of candidate genes identified from primary screening

We chose the 216 strongest candidates based on transposon de-repression, and repeated our experimental workflow by re-crossing the same dsRNA line followed by multiplexed qPCR.

Whenever available, we extended our analysis by including an independent RNAi line (dsRNA or shRNA, derived from either the VDRC or TRiP stock centers) targeting a different region of the candidate gene. In addition to the four transposons, we also probed the levels of two genes highly expressed in germline cells (*nos*, *yTub37c*). For better comparison across data sets, we calculated all expression changes relative to the average of ten independent negative control knockdowns (6x *w*, 3x *yb*, 1x *GFP*), and compared to the average of two *armi* control knockdowns included on each plate. Furthermore, we analyzed potential fertility defects by counting the number of larvae and pupae. For an improved overview, heat maps summarizing all assayed parameters are shown only for the 100 strongest hits (Figure 3). Overall, we found significant overlap between our primary screen data, the rescreening using the identical dsRNA line, and an independent RNAi line, evidencing the high reproducibility of our data. Notably, compromised fertility correlates either with reduced expression of the germline markers *nos* and *yTub37c*, or with general transposon de-repression with changes similar to *armi* knockdowns.

Our re-screening validated the identification of all known piRNA pathway components that have been reported to affect the germline pathway, with the exception of Krimper, for which no dsRNA line was available, and the *Drosophila* SETDB1 ortholog, Egg. In addition to genes already implicated in the piRNA pathway, our screen uncovered numerous novel candidates that cause dramatic transposon de-repression, often accompanied by fertility defects, when depleted from germline cells. The new candidate with the highest average level transposon up-regulation, *deadlock* (*del*), was previously reported as gene important for germline maintenance and female fertility, with lesions resulting in defects during early oogenesis (Schupbach and Wieschaus, 1991; Wehr et al., 2006). Another gene that dramatically de-repressed all four measured transposable elements was *CG2183*, which we named *GASZ* after its nearest vertebrate counterpart (Yan et al., 2002). *Drosophila* *GASZ* shares the ankyrin repeats and a predicted sterile alpha motif of vertebrate *GASZ* (Figure S3A). Murine *GASZ* is a nuage component, with its loss resulting in transposon de-repression, sterility and reduced piRNA levels (Ma et al., 2009). Another strong hit, *CG3893*, which caused significant de-repression of all tested transposons, was also identified as a major factor for piRNA-mediated silencing in somatic tissues (Muerdter et al.). Another as yet-uncharacterized candidate, *CG9754*, is predicted to code for a nuclear protein without conserved domains, and its depletion results in dramatic up-regulation of all tested transposons. Last, *Ars2*, was previously shown to impact the biogenesis of miRNAs and siRNAs (Gruber et al., 2009; Sabin et al., 2009), but no function in the piRNA pathway was reported. In all, we identified a total of 74 factors with pronounced effects on all transposons tested.

Placement of candidate hits within the piRNA pathway

To characterize molecular functions of *GASZ* and *Del*, we first studied the subcellular localization pattern of selected piRNA pathway components upon germline-specific knockdown or in mutant animals. Depletion of *w* resulted in retention of the expected localization of all investigated proteins: Piwi was prominent within the nurse cell nuclei, whereas Aub and AGO3 were both enriched in nuage granules, and *Armi* was detected in diffuse perinuclear structures reminiscent of nuage (Figure 4A) (Brennecke et al., 2007; Cox et al., 1998; Cox et al., 2000; Gunawardane et al., 2007; Lim and Kai, 2007; Nishida et al., 2007; Saito et al., 2010; Saito et al., 2006). A dsRNA specific to *armi* resulted in loss of *Armi* protein below detectable levels in germline cells, while *Armi* staining in the Yb-bodies of adjacent follicle cells remained intact. Consistent with its function in primary piRNA biogenesis, depletion of *Armi* caused the redistribution of Piwi from nurse cell nuclei, but had no effect on the localization of Aub and AGO3 (Figure 4A). Upon knockdown of *gasz*, nuclear localization of Piwi was severely compromised, whereas Aub and AGO3 appeared

normal. Interestingly, we also observed a redistribution of Armi from nuage granules into cytoplasmic speckles, suggesting that GASZ might act in primary piRNA biogenesis (Figure 4A). Depletion of *del*, in contrast, did not affect Piwi, while Aub was re-distributed from nuage (data not shown). These results were confirmed by analysis of *del* mutant females, which showed delocalization of Aub and AGO3 from nuage, compared to their heterozygote siblings (Figure 4B). Consistent with our knockdown experiments the nuclear localization of Piwi was preserved. Thus, *del* could act specifically in the ping-pong cycle.

GASZ and Del affect different steps of piRNA biogenesis

Transposon de-repression, reduced fertility, and disturbed PIWI-clade protein localization are hallmarks of piRNA pathway mutants. To directly probe possible effects on piRNA levels, we cloned and sequenced small RNA libraries from ovaries with germline-specific depletion of GASZ or Del. For comparison, we also prepared small RNA libraries from germline knockdowns of several known piRNA pathway factors. We normalized small RNAs to the number of unique piRNA reads derived from the *flam* cluster, which were not affected by germline knockdowns. Germline-specific depletion of Yb behaved highly similar to *w* knockdowns and caused no alterations in piRNA populations, whereas all other dsRNAs resulted in significantly reduced *42AB*-derived piRNA levels (Figure 5A). Consequently, while the fraction of reads corresponding to miRNAs was indistinguishable between *w* and *yb* knockdowns, slightly increased miRNA fractions coincided with reduced piRNA levels in all other knockdowns (Figure 5A). 23- to 29-nt piRNA levels of reads uniquely derived from the *42AB* locus, in contrast, were dramatically reduced upon knockdown of *armi* (35.3x), *gasz* (57.4x), *spn-E* (26.9x), *aub* (6.0x), or *del* (13.3x), as shown by length profiles. The abundance of endo-siRNAs, which are produced and loaded by independent machineries, was similar for all knockdowns with a marginal increase observed in cases where piRNAs were depleted from the small RNA cloning pool (e.g. *gasz* knockdown). Notably, knockdown of *del* resulted in a near-complete loss of endo-siRNAs, indicating an effect on piRNA precursor transcripts.

Similar piRNA losses were observed for sequences derived from other germline-active clusters (Figure 5C). Interestingly, piRNA levels derived from the single-stranded cluster *20A* were dramatically reduced in all knockdowns besides *del* (and the controls *w* and *yb*). Similar defects have been reported for flies mutant for Rhi and Cuff, both shown important for germline-cluster transcription (Klattenhoff et al., 2009; Pane et al., 2011). We generated GFP-Del transgenic flies and found that, like Rhi and Cuff, Del exhibits a punctate nuclear localization pattern (Figure S3B). Furthermore, depletion of GASZ in follicle cells using the *tj*-GAL4 driver, resulted in greatly reduced levels of piRNAs originating from *flam* (or the *tj* 3' UTR), similar to the effects of Armi depletion, when compared to *w* or *spn-E* control knockdowns (Figure S4B and C).

Next, we analyzed the effect of depleting either of these factors on the ping-pong signature, which is defined as the frequency of reads from opposite strands overlapping by 10-nt, of *42AB*-derived piRNAs (Figure 5B). Knockdown of *armi* and *gasz* resulted in increased ping-pong signatures, compared to *w* or *yb* knockdown, whereas depletion of Spn-E and Aub, known components of the ping-pong amplification loop, as well as Del resulted in significantly reduced frequency of ping-pong pairs (Figure 5B). The reciprocal effects on ping-pong signatures observed in *gasz* and *del* knockdowns further support the conjecture that these genes play roles specific to primary and secondary piRNA biogenesis pathways, respectively. Moreover, the product of a GFP-GASZ transgene localizes to perinuclear structures in the female germline and overlaps with staining for mitochondria in OSS cells, with both sites characteristic for primary piRNA biogenesis components in *Drosophila* (Figure S3C and D) (Olivieri et al., 2012; Preall et al., 2012).

We also analyzed effects on piRNAs corresponding to a set of 80 established transposons (Figure 5D). Based on previous data, we separated these elements into those that dominate in somatic cells, intermediate transposons and mobile elements predominantly active in germline cells (Malone et al., 2009). In comparison to *w* knockdown, depletion of Yb caused only minimal changes in piRNAs derived from any transposon (Figure S4A, top). All other knockdowns showed varying reduction of piRNA levels from germline dominant elements. Intermediate transposons showed mildly reduced piRNA levels, and soma-enriched mobile elements were not changed significantly (less than 2-fold). Levels of germline dominant piRNAs were affected to similar extent upon knockdown of *armi* and *gasz*, suggesting related functions in primary biogenesis (Figure S4A, middle). Knockdown of *armi* and *aub* resulted in highly correlating piRNA levels (Figure S4A, bottom), in agreement with Aub receiving inputs from primary biogenesis, but despite unaltered Aub localization upon *armi* knockdown (Figure 4).

These similar relations were confirmed by mapping piRNAs over the LTR transposon *batumi*, which is predominantly active in the germline lineage (Figure 5E). While knockdown of *yb* showed similar piRNA levels to *w* controls, depletion of *Armi* and *GASZ* resulted in severe reduction of piRNAs, with some ping-pong-derived pairs persisting. Knockdown of *spn-E*, in contrast, caused a dramatic loss of piRNA populations. Depletion of *Aub* resulted in significantly reduced piRNA levels, with the remaining sequences probably associated with the other PIWI-clade proteins *Piwi* and *AGO3*. Knockdown of *del* also showed severely reduced levels of piRNAs matching the *batumi* transposon, but had distinct patterns compared to all other knockdowns.

Differential silencing requirements for distinct transposon types

Transposons are cataloged based on their sequence, transposition strategy, and replication intermediates and can be separated coarsely into DNA elements and retrotransposons (Slotkin and Martienssen, 2007). The latter are further subdivided into LTR transposons (including *blood* and *burdock*), and non-LTR elements to which the LINE-like *HeTA* and *TAHRE* transposons belong. Each element class displays its own unique genome and life cycle within the fly, thus it is likely that transposon-specific adaptations evolved for efficient silencing of each type. To analyze whether specific genes are only required for repression of certain transposons, we compared de-silencing phenotypes between elements. As expected by their similar replication cycle, *z*-scores for *HeTA* and *TAHRE* highly correlated amongst the top 500 genes scored as hits ($R^2 = 0.62$) (Figure 6A). In contrast, correlations between *HeTA* and the LTR elements *blood* (Figure 6B) or *burdock* (Figure S5A) are much weaker ($R^2 = 0.08$ and 0.01 , respectively), probably reflecting important differences in the silencing determinants for these elements. Importantly, all factors known to affect piRNA biogenesis showed strong transposon de-repression for all four elements, with an ensemble average *z*-score of $-3.66 (\pm 0.57)$. Thus, knockdowns that robustly de-silence all four elements are highly enriched for core piRNA pathway components. After inspecting our secondary screen (Figure 3) as a filter for false positives, we can classify 17 new genes with an average transposon *z*-score in this range, including both *gasz* and *del*, that to our knowledge have not been previously linked to piRNA-mediated silencing.

One of the strengths of our screen setup is that it also reveals an array of factors that participate in silencing individual mobile elements or transposon families, but lay outside the core piRNA pathway. For example, *CG5694* and *Isd1*, also known as *Su(var)3-3*, are critical for silencing both *HeTA* and *TAHRE*, but have no effect on *burdock* or *blood* (compare Figure 6A with 6B and Figure S5A). Interestingly, *Isd1* codes for a histone demethylase, suggesting a specific requirement for certain chromatin modifiers in suppressing telomeric, LINE-like elements. A comparison of *blood* and *burdock* revealed a relatively weak correlation between de-silencing of these elements ($R^2 = 0.07$, Figure S5B).

Notably, *Actr13E* and *U2A* were specifically required for the suppression of *blood*, with little to no effect on the other tested transposons, while the putative RNA-binding protein *swm* appeared specific for *burdock* silencing. Comparatively few disparities between *HeTA* and *TAHRE* silencing were observed and the *z*-score correlation between these elements was significantly higher than any other pairwise combination, this suggesting that the mechanisms by which these elements are controlled are nearly identical.

To more deeply investigate the spectrum of transposable elements silenced by a given gene, we analyzed the mRNA complement of *nos*-Gal4 driven knockdown ovaries for a number of known piRNA genes and novel candidates by RNAseq. As expected, depletion of primary piRNA biogenesis factors such as Piwi, Shu, Armi, or Zuc resulted in the strongest de-silencing of the widest variety of element classes relative to *w* controls (Figure 6C). We note that *GASZ* also silences a broad spectrum of elements, in keeping with our assessment of it as a putative primary biogenesis factor based on small RNA cloning and localization studies. Factors involved in ping-pong amplification, expression of specific piRNA clusters, or other as-yet undescribed ‘effector’ functions of the pathway show robust de-silencing of a narrower subset of elements, most notably *HeTA*, *TAHRE*, *blood*, and *burdock*, which further supports that measurement of these elements provided the optimal sensitivity with regards to our primary screen. As expected, *del* knockdown also resulted in dramatic up-regulation of many elements in addition to those probed by the screen. We also independently profiled the silencing spectrum of *CG3893* (Muerdter et al.), which is among the broadest and strongest in our analysis and further confirms this gene as a core component of piRNA-mediated transposon silencing. Finally, the element specificity of certain candidates observed in our primary screen was born out here, with *U2A* showing exquisite specificity for *blood* and *Ars2* only displaying notable de-silencing among LINE-like elements.

Discussion

With very few exceptions, piRNA pathway components were originally identified by classic reverse genetic screens and only linked to piRNA biogenesis or effector mechanisms through later experiments (Schupbach and Wieschaus, 1989, 1991). Forward genetic approaches have been powerful in identifying new pathway components in somatic tissues of *Drosophila*, and were recently engaged in mini-screens to probe the requirement of known factors for somatic piRNA silencing or to analyze Tudor and FKBP protein biology in somatic and germline cells (Handler et al., 2011; Olivieri et al., 2010; Preall et al., 2012). However, to date, no systematic screen has been published that aimed to find novel components of the much more complex germline piRNA pathway. Here, we report an *in vivo* screen carried out in germ cells of the *Drosophila* ovary designed to uncover new core piRNA machinery as well as factors involved in general mechanisms of transposon silencing. Overall, we identified 74 genes that severely affect silencing of a set of four transposons. Importantly, of 17 known piRNA pathway components included in the screen, all but *Egg* were present in this enriched set, providing a powerful validation of the screen approach. While germline depletion of core piRNA components generally permits normal ovarian development, genes with essential functions in germ cell viability are expected to be underrepresented by our hits due to masking of the qPCR phenotype.

By measuring de-silencing of an array of transposon types, we were able to further narrow down our candidate list to factors that are very likely to be core components of the piRNA response. Knockdowns of known piRNA related genes also share the properties of inducing sterility while grossly maintaining the integrity of the germline, as measured by specific markers *nos* and *yTub37c*. Our screen identifies ~15 additional genes that show properties exactly like established piRNA genes. Among these, we confirmed *GASZ* as a primary

biogenesis factor that likely acts upstream of *Armi*. In addition, we provide evidence that *Del* is a new piRNA component that participates in secondary biogenesis evidenced by reduced ping-pong amplification. Consistent with this observation, loss of *Del* displaces *Aub* and *AGO3* from nuage while retaining nuclear localization of *Piwi*. The protein product of *del* is not conserved outside of *Drosophilids* and contains no predicted domains or motifs, leaving its molecular role in secondary piRNA production an open question, though given the similarity to *cuff* and *rhi* knockdown phenotypes it is tempting to speculate that *Del* affects transcription of dual-strand clusters (Klattenhoff et al., 2009; Pane et al., 2011). While we have confidently added two new factors to the milieu of the piRNA biogenesis machinery, further experiments will be necessary to discriminate piRNA producers from effectors amongst the remainder of our candidate core components.

Simultaneously with this effort, our lab also conducted an independent, genome-wide RNAi screen for primary piRNA components in *Drosophila* OSS cells (Muerdter et al.). This complementary screen reports several of the same components identified here, among which are the putative primary biogenesis factor *GASZ*, the likely effector step gene *CG3893* (now named *Asterix*), and several additional candidates with yet-to-be-determined functions that include the nuclear protein *CG9754*, and the Egg co-factor *windei*. Somatic and germline piRNA pathways face distinct threats with regards to transposon activation, and thus it is to be expected that many factors will be unique to each lineage. Furthermore, earlier studies suggested specific adaptations of related components within either lineage, with *Yb* (soma) and *BoYb/SoYb* (germline) being the most prominent examples (Handler et al., 2011). Among the overlap, we expect to find primarily genes involved in the biogenesis of cluster-derived primary piRNAs (transcription, precursor export, import of *Piwi*, or transcriptional activation of clusters by *Piwi*), though the clusters in question differ significantly. Indeed, both screens identify numerous components or subunits of established cellular pathways and complexes like the exon-junction complex (EJC), the nonspecific lethal (NSL) complex, the SUMOylation machinery, and general RNA metabolism and/or export factors (Figure 7). Additionally, each tissue may utilize similar general effector mechanisms coupled to *Piwi*-bound piRNAs, as highlighted by the common requirement of *CG3893/Asterix*. Of all genes essential for proper transposon silencing in both tissues, we recovered six known piRNA pathway components (*Piwi*, *Armi*, *Zuc*, *Shu*, *Vret*, *Mael*), as well as 26 novel factors that fall into the categories described above and await further characterization with respect to their mechanistic impact on transposon repression.

Clues to silencing effector mechanisms

Small RNA-based gene silencing pathways have been suggested to regulate targets at the transcriptional level in a variety of organisms, including *Drosophila*. In particular, piRNA-mediated silencing has been shown to promote the deposition of repressive H3K9me3 marks at certain transposon loci (Klenov et al., 2007; Le Thomas et al., 2013; Rozhkov et al., 2013; Sienski et al., 2012). Curiously, the same mark has also been shown to be essential for the robust transcription of piRNA clusters (Rangan et al., 2011). As a nuclear protein, *Piwi* is the principal orchestrator of such chromatin modifications, but its cohort of co-repressor proteins and further mechanistic detail remain largely mysterious. While the mechanism of transcriptional-level silencing by small RNAs has been extensively characterized in fission yeast, most of the key players are not conserved in *Drosophila*. This screen classifies several known regulators of transcriptional output as “strong” transposon silencers, including the H3K9 methyltransferase *Su(var)3-9*, *HPI/Su(var)205*, *His2Av*, *mof*, and *TfIIA-S*. A significant number of further chromatin-related genes seem to exert an effect on individual elements, most notably the putative H3K4-specific demethylase *Lsd1*.

In addition to uncovering novel, uncharacterized factors in the piRNA pathway, our screen also reveals that certain established multi-subunit complexes play important (but potentially

indirect) roles in transposon silencing. For instance, all three components of the nuclear cap-binding complex (Ars2, cbp80, and cbp20) exhibit strong de-silencing of multiple elements upon knockdown (Figure 7). This complex has been implicated in mRNA quality control and surveillance in other systems, to which we now add a critical and general function in transposon regulation (Gruber et al., 2009; Maquat, 2004; Sabin et al., 2009). We also observed de-repression of at least one element in each of the components of the THO complex, which has been implicated in a number of nuclear processes including mRNA splicing, export, and surveillance (Rehwinkel et al., 2004). Last, we note substantial enrichment of components belonging to the EJC, the NSL complex, the SUMOylation machinery, as well as the macromolecular H3K4 methyltransferase, dSet1/COMPASS (Chang et al., 2007; Mohan et al., 2011; Raja et al., 2010; Talamillo et al., 2008; Tange et al., 2005). As functional characterization of the *Drosophila* genome expands, no doubt further genetic and physical relationships between poorly annotated screen hits will reveal themselves.

Transposable elements that threaten the germline genome can be found within all classes of chromatin, and are thus embedded within a variety of molecular contexts. It seems plausible that the specific effectors modulating a given element insertion are a function of chromatin context, with Piwi acting as a general purpose local silencing trigger by targeting a nascent transcript and providing a cooperative binding surface for a limited set of nearby co-repressors. Another factor that may contribute to the variability we observe across candidates and element classes are the idiosyncrasies of a given element's life cycle and transposition strategy. The telomeric transposons *HeTA* and *TAHRE*, for example, play an important cellular role that is presumably maintained in a delicate balance: too little activity could lead to telomere shortening and chromosomal aberrations, while too much could lead to mutagenic levels of transposition. These elements are very likely regulated by a number of cellular processes independent of the piRNA pathway. Similarly, many LTR elements exploit host machinery to assemble into virus-like particles. Recognition of structures harboring transposon RNAs may be a key strategy employed by the piRNA machinery for finding its targets.

In summary, our transcriptome-wide RNAi screen has provided a rich resource for further study, comprising a set of genes involved in transposable element suppression in the *Drosophila* female germline. Our aim was to produce a comprehensive list of core components of the primary and secondary piRNA pathways, and indeed we have confirmed two hits as such with many more yet to pursue in more detail. A second benefit of this dataset is to provide insights into the cellular niche occupied by a subset of highly abundant transposable elements in *Drosophila*. Understanding how an individual transposable element exploits its host machinery is likely to lead to important discoveries regarding general mechanisms of gene silencing and RNA trafficking. Most importantly, this study in combination with the accompanying somatic screen advances our knowledge of the key players in the piRNA pathway, with the ultimate goal of having the blueprints for building a fully operationally piRNA silencing machine nearly in hand.

Experimental Procedures

Fly stocks and husbandry

Details on fly stocks and husbandry as well as the screening procedure are given in the Extended Experimental Procedures.

RNA isolation, reverse transcription, qPCR

A detailed protocol is provided in the Extended Experimental Procedures.

Immunofluorescence

The immunofluorescence experiments were carried out as described (Preall et al., 2012), details are given in the Extended Experimental Procedures. Anti-Piwi and anti-AGO3 were generated in the Hannon laboratory (Brennecke et al., 2007). Anti-Aub and anti-Armi were gifts from Mikiko Siomi (Nishida et al., 2007; Saito et al., 2010). Secondary antibodies (AlexaFluor-488 and -568) were purchased from Invitrogen.

Small RNA libraries and bioinformatic analysis

Small RNA libraries were constructed similar as described (Brennecke et al., 2007), with slightly modified adapters that enabled multiplexed sequencing. Libraries constructed for this study are listed in the Extended Experimental Procedures.

The analysis of small RNA libraries was performed similar as described (Czech et al., 2008; Preall et al., 2012). Detailed information is provided in the Extended Experimental Procedures.

RNAseq experiments and transcriptome analysis

A detailed description of RNAseq experiments and computational transcriptome analysis is given in the Extended Experimental Procedures.

Supplementary Material

Refer to Web version on PubMed Central for supplementary material.

Acknowledgments

We thank members of the Hannon laboratory for helpful discussion, Maria Mosquera and Steven Sau for help with fly husbandry and qPCR, and Assaf Gordon, Simon Knott and Felix Muerdter for computational support. We thank the VDRC, TRiP and Bloomington stock centers for fly stocks. For part of this work, BC was supported by a PhD fellowship from the Boehringer Ingelheim Fonds. JP is supported by the American Cancer Society (award number 121614-PF-11-277-01-RMC). This work was supported in part by grants from the NIH and a kind gift from Kathryn W. Davis. GJH. is an investigator of the HHMI.

References

- Anand A, Kai T. The tudor domain protein kumo is required to assemble the nuage and to generate germline piRNAs in *Drosophila*. *Embo J*. 2012; 31:870–882. [PubMed: 22157814]
- Aravin A, Gaidatzis D, Pfeffer S, Lagos-Quintana M, Landgraf P, Iovino N, Morris P, Brownstein MJ, Kuramochi-Miyagawa S, Nakano T, et al. A novel class of small RNAs bind to MILI protein in mouse testes. *Nature*. 2006; 442:203–207. [PubMed: 16751777]
- Brennecke J, Aravin AA, Stark A, Dus M, Kellis M, Sachidanandam R, Hannon GJ. Discrete small RNA-generating loci as master regulators of transposon activity in *Drosophila*. *Cell*. 2007; 128:1089–1103. [PubMed: 17346786]
- Brennecke J, Malone CD, Aravin AA, Sachidanandam R, Stark A, Hannon GJ. An epigenetic role for maternally inherited piRNAs in transposon silencing. *Science*. 2008; 322:1387–1392. [PubMed: 19039138]
- Chang YF, Imam JS, Wilkinson MF. The nonsense-mediated decay RNA surveillance pathway. *Annu Rev Biochem*. 2007; 76:51–74. [PubMed: 17352659]
- Cox DN, Chao A, Baker J, Chang L, Qiao D, Lin H. A novel class of evolutionarily conserved genes defined by piwi are essential for stem cell self-renewal. *Genes Dev*. 1998; 12:3715–3727. [PubMed: 9851978]
- Cox DN, Chao A, Lin H. piwi encodes a nucleoplasmic factor whose activity modulates the number and division rate of germline stem cells. *Development*. 2000; 127:503–514. [PubMed: 10631171]

- Czech B, Malone CD, Zhou R, Stark A, Schlingeheyde C, Dus M, Perrimon N, Kellis M, Wohlschlegel JA, Sachidanandam R, et al. An endogenous small interfering RNA pathway in *Drosophila*. *Nature*. 2008; 453:798–802. [PubMed: 18463631]
- Dietz G, Chen D, Schnorrer F, Su KC, Barinova Y, Fellner M, Gasser B, Kinsey K, Oppel S, Scheiblaue S, et al. A genome-wide transgenic RNAi library for conditional gene inactivation in *Drosophila*. *Nature*. 2007; 448:151–156. [PubMed: 17625558]
- Girard A, Sachidanandam R, Hannon GJ, Carmell MA. A germline-specific class of small RNAs binds mammalian Piwi proteins. *Nature*. 2006; 442:199–202. [PubMed: 16751776]
- Gruber JJ, Zatechka DS, Sabin LR, Yong J, Lum JJ, Kong M, Zong WX, Zhang Z, Lau CK, Rawlings J, et al. *Ars2* links the nuclear cap-binding complex to RNA interference and cell proliferation. *Cell*. 2009; 138:328–339. [PubMed: 19632182]
- Gunawardane LS, Saito K, Nishida KM, Miyoshi K, Kawamura Y, Nagami T, Siomi H, Siomi MC. A slicer-mediated mechanism for repeat-associated siRNA 5' end formation in *Drosophila*. *Science*. 2007; 315:1587–1590. [PubMed: 17322028]
- Handler D, Olivieri D, Novatchkova M, Gruber FS, Meixner K, Mechtler K, Stark A, Sachidanandam R, Brennecke J. A systematic analysis of *Drosophila* TUDOR domain-containing proteins identifies Vreteno and the Tdrd12 family as essential primary piRNA pathway factors. *Embo J*. 2011; 30:3977–3993. [PubMed: 21863019]
- Kawaoka S, Izumi N, Katsuma S, Tomari Y. 3' end formation of PIWI-interacting RNAs in vitro. *Mol Cell*. 2011; 43:1015–1022. [PubMed: 21925389]
- Khurana JS, Theurkauf W. piRNAs, transposon silencing, and *Drosophila* germline development. *J Cell Biol*. 2010; 191:905–913. [PubMed: 21115802]
- Klattenhoff C, Xi H, Li C, Lee S, Xu J, Khurana JS, Zhang F, Schultz N, Koppetsch BS, Nowosielska A, et al. The *Drosophila* HP1 homolog Rhino is required for transposon silencing and piRNA production by dual-strand clusters. *Cell*. 2009; 138:1137–1149. [PubMed: 19732946]
- Klenov MS, Lavrov SA, Stolyarenko AD, Ryazansky SS, Aravin AA, Tuschl T, Gvozdev VA. Repeat-associated siRNAs cause chromatin silencing of retrotransposons in the *Drosophila melanogaster* germline. *Nucleic Acids Res*. 2007; 35:5430–5438. [PubMed: 17702759]
- Lau NC, Robine N, Martin R, Chung WJ, Niki Y, Berezikov E, Lai EC. Abundant primary piRNAs, endo-siRNAs, and microRNAs in a *Drosophila* ovary cell line. *Genome Res*. 2009; 19:1776–1785. [PubMed: 19541914]
- Le Thomas A, Rogers AK, Webster A, Marinov GK, Liao SE, Perkins EM, Hur JK, Aravin AA, Toth KF. Piwi induces piRNA-guided transcriptional silencing and establishment of a repressive chromatin state. *Genes Dev*. 2013; 27:390–399. [PubMed: 23392610]
- Li C, Vagin VV, Lee S, Xu J, Ma S, Xi H, Seitz H, Horwich MD, Syrzycka M, Honda BM, et al. Collapse of germline piRNAs in the absence of Argonaute3 reveals somatic piRNAs in flies. *Cell*. 2009; 137:509–521. [PubMed: 19395009]
- Lim AK, Kai T. Unique germ-line organelle, nuage, functions to repress selfish genetic elements in *Drosophila melanogaster*. *Proc Natl Acad Sci U S A*. 2007; 104:6714–6719. [PubMed: 17428915]
- Ma L, Buchold GM, Greenbaum MP, Roy A, Burns KH, Zhu H, Han DY, Harris RA, Coarfa C, Gunaratne PH, et al. GASZ is essential for male meiosis and suppression of retrotransposon expression in the male germline. *PLoS Genet*. 2009; 5:e1000635. [PubMed: 19730684]
- Malone CD, Brennecke J, Dus M, Stark A, McCombie WR, Sachidanandam R, Hannon GJ. Specialized piRNA pathways act in germline and somatic tissues of the *Drosophila* ovary. *Cell*. 2009; 137:522–535. [PubMed: 19395010]
- Malone CD, Hannon GJ. Small RNAs as guardians of the genome. *Cell*. 2009; 136:656–668. [PubMed: 19239887]
- Maquat LE. Nonsense-mediated mRNA decay: splicing, translation and mRNP dynamics. *Nat Rev Mol Cell Biol*. 2004; 5:89–99. [PubMed: 15040442]
- Mohan M, Herz HM, Smith ER, Zhang Y, Jackson J, Washburn MP, Florens L, Eissenberg JC, Shilatifard A. The COMPASS family of H3K4 methylases in *Drosophila*. *Mol Cell Biol*. 2011; 31:4310–4318. [PubMed: 21875999]
- Niki Y, Yamaguchi T, Mahowald AP. Establishment of stable cell lines of *Drosophila* germ-line stem cells. *Proc Natl Acad Sci U S A*. 2006; 103:16325–16330. [PubMed: 17056713]

- Nishida KM, Saito K, Mori T, Kawamura Y, Nagami-Okada T, Inagaki S, Siomi H, Siomi MC. Gene silencing mechanisms mediated by Aubergine piRNA complexes in *Drosophila* male gonad. *Rna*. 2007; 13:1911–1922. [PubMed: 17872506]
- Olivieri D, Senti KA, Subramanian S, Sachidanandam R, Brennecke J. The Cochaperone Shutdown Defines a Group of Biogenesis Factors Essential for All piRNA Populations in *Drosophila*. *Mol Cell*. 2012
- Olivieri D, Sykora MM, Sachidanandam R, Mechtler K, Brennecke J. An in vivo RNAi assay identifies major genetic and cellular requirements for primary piRNA biogenesis in *Drosophila*. *Embo J*. 2010; 29:3301–3317. [PubMed: 20818334]
- Pane A, Jiang P, Zhao DY, Singh M, Schupbach T. The Cutoff protein regulates piRNA cluster expression and piRNA production in the *Drosophila* germline. *Embo J*. 2011; 30:4601–4615. [PubMed: 21952049]
- Patil VS, Kai T. Repression of retroelements in *Drosophila* germline via piRNA pathway by the Tudor domain protein Tejas. *Curr Biol*. 2010; 20:724–730. [PubMed: 20362446]
- Preall JB, Czech B, Guzzardo PM, Muerdter F, Hannon GJ. shutdown is a component of the *Drosophila* piRNA biogenesis machinery. *Rna*. 2012; 18:1446–1457. [PubMed: 22753781]
- Qi H, Watanabe T, Ku HY, Liu N, Zhong M, Lin H. The Yb body, a major site for Piwi-associated RNA biogenesis and a gateway for Piwi expression and transport to the nucleus in somatic cells. *J Biol Chem*. 2011; 286:3789–3797. [PubMed: 21106531]
- Raja SJ, Charapitsa I, Conrad T, Vaquerizas JM, Gebhardt P, Holz H, Kadlec J, Fraterman S, Luscombe NM, Akhtar A. The nonspecific lethal complex is a transcriptional regulator in *Drosophila*. *Mol Cell*. 2010; 38:827–841. [PubMed: 20620954]
- Rangan P, Malone CD, Navarro C, Newbold SP, Hayes PS, Sachidanandam R, Hannon GJ, Lehmann R. piRNA production requires heterochromatin formation in *Drosophila*. *Curr Biol*. 2011; 21:1373–1379. [PubMed: 21820311]
- Rehwinkel J, Herold A, Gari K, Kocher T, Rode M, Ciccarelli FL, Wilm M, Izaurralde E. Genome-wide analysis of mRNAs regulated by the THO complex in *Drosophila melanogaster*. *Nat Struct Mol Biol*. 2004; 11:558–566. [PubMed: 15133499]
- Rozhkov NV, Hammell M, Hannon GJ. Multiple roles for Piwi in silencing *Drosophila* transposons. *Genes Dev*. 2013; 27:400–412. [PubMed: 23392609]
- Sabin LR, Zhou R, Gruber JJ, Lukinova N, Bambina S, Berman A, Lau CK, Thompson CB, Cherry S. Ars2 regulates both miRNA- and siRNA- dependent silencing and suppresses RNA virus infection in *Drosophila*. *Cell*. 2009; 138:340–351. [PubMed: 19632183]
- Saito K, Inagaki S, Mituyama T, Kawamura Y, Ono Y, Sakota E, Kotani H, Asai K, Siomi H, Siomi MC. A regulatory circuit for piwi by the large Maf gene traffic jam in *Drosophila*. *Nature*. 2009; 461:1296–1299. [PubMed: 19812547]
- Saito K, Ishizu H, Komai M, Kotani H, Kawamura Y, Nishida KM, Siomi H, Siomi MC. Roles for the Yb body components Armitage and Yb in primary piRNA biogenesis in *Drosophila*. *Genes Dev*. 2010; 24:2493–2498. [PubMed: 20966047]
- Saito K, Nishida KM, Mori T, Kawamura Y, Miyoshi K, Nagami T, Siomi H, Siomi MC. Specific association of Piwi with rasiRNAs derived from retrotransposon and heterochromatic regions in the *Drosophila* genome. *Genes Dev*. 2006; 20:2214–2222. [PubMed: 16882972]
- Schupbach T, Wieschaus E. Female sterile mutations on the second chromosome of *Drosophila melanogaster*. I. Maternal effect mutations. *Genetics*. 1989; 121:101–117. [PubMed: 2492966]
- Schupbach T, Wieschaus E. Female sterile mutations on the second chromosome of *Drosophila melanogaster*. II. Mutations blocking oogenesis or altering egg morphology. *Genetics*. 1991; 129:1119–1136. [PubMed: 1783295]
- Senti KA, Brennecke J. The piRNA pathway: a fly's perspective on the guardian of the genome. *Trends Genet*. 2010; 26:499–509. [PubMed: 20934772]
- Sienski G, Donertas D, Brennecke J. Transcriptional silencing of transposons by Piwi and maelstrom and its impact on chromatin state and gene expression. *Cell*. 2012; 151:964–980. [PubMed: 23159368]
- Siomi MC, Sato K, Pezic D, Aravin AA. PIWI-interacting small RNAs: the vanguard of genome defence. *Nat Rev Mol Cell Biol*. 2011; 12:246–258. [PubMed: 21427766]

- Slotkin RK, Martienssen R. Transposable elements and the epigenetic regulation of the genome. *Nat Rev Genet.* 2007; 8:272–285. [PubMed: 17363976]
- Szakmary A, Reedy M, Qi H, Lin H. The Yb protein defines a novel organelle and regulates male germline stem cell self-renewal in *Drosophila melanogaster*. *J Cell Biol.* 2009; 185:613–627. [PubMed: 19433453]
- Talamillo A, Sanchez J, Barrio R. Functional analysis of the SUMOylation pathway in *Drosophila*. *Biochem Soc Trans.* 2008; 36:868–873. [PubMed: 18793153]
- Tange TO, Shibuya T, Jurica MS, Moore MJ. Biochemical analysis of the EJC reveals two new factors and a stable tetrameric protein core. *Rna.* 2005; 11:1869–1883. [PubMed: 16314458]
- Wang SH, Elgin SC. *Drosophila* Piwi functions downstream of piRNA production mediating a chromatin-based transposon silencing mechanism in female germ line. *Proc Natl Acad Sci U S A.* 2011; 108:21164–21169. [PubMed: 22160707]
- Wehr K, Swan A, Schupbach T. Deadlock, a novel protein of *Drosophila*, is required for germline maintenance, fusome morphogenesis and axial patterning in oogenesis and associates with centrosomes in the early embryo. *Dev Biol.* 2006; 294:406–417. [PubMed: 16616913]
- Yan W, Rajkovic A, Viveiros MM, Burns KH, Eppig JJ, Matzuk MM. Identification of Gasz, an evolutionarily conserved gene expressed exclusively in germ cells and encoding a protein with four ankyrin repeats, a sterile-alpha motif, and a basic leucine zipper. *Mol Endocrinol.* 2002; 16:1168–1184. [PubMed: 12040005]
- Zamparini AL, Davis MY, Malone CD, Vieira E, Zavadil J, Sachidanandam R, Hannon GJ, Lehmann R. Vreteno, a gonad-specific protein, is essential for germline development and primary piRNA biogenesis in *Drosophila*. *Development.* 2011; 138:4039–4050. [PubMed: 21831924]
- Zhang Z, Xu J, Koppetsch BS, Wang J, Tipping C, Ma S, Weng Z, Theurkauf WE, Zamore PD. Heterotypic piRNA Ping-Pong requires qin, a protein with both E3 ligase and Tudor domains. *Mol Cell.* 2011; 44:572–584. [PubMed: 22099305]

Highlights

- Proper transposon silencing in *Drosophila* germ cells depends on at least 74 genes
- Screening identifies novel piRNA biogenesis factors and effector proteins
- Silencing of distinct transposons requires different mechanisms

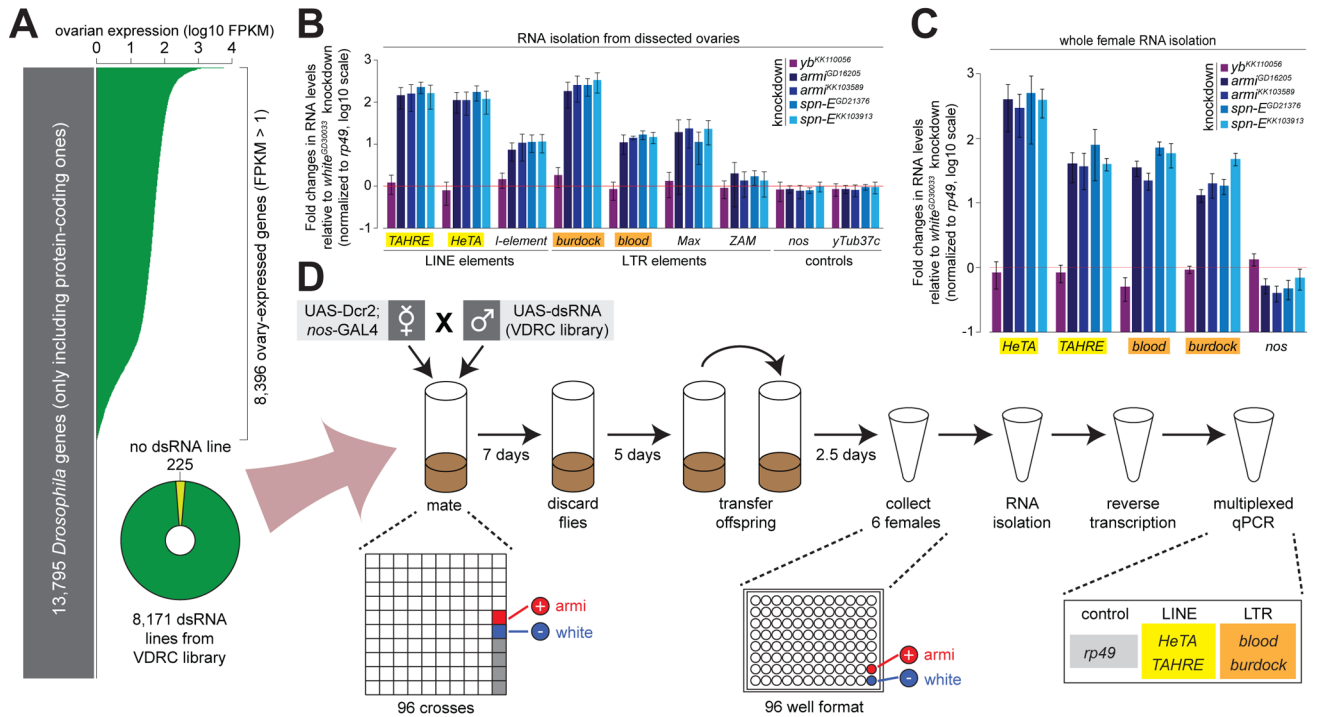


Figure 1. Screen workflow and summary of preliminary experiments

(A) Relative expression levels of protein-coding genes in *Drosophila melanogaster* are shown for ovarian RNAseq data as histogram. Green bars highlight ovary-expressed genes with FPKM > 1. Doughnut diagram shows screened genes where dsRNA line was available from the VDRC. (B) Histograms show the relative expression levels of indicated transposons detected in ovaries that express dsRNA against *yb*, *armi* or *spn-E* in germline cells. Fold changes are relative to knockdown of *w* (indicated by red line). Measurements were carried out on ovary-dissected total RNA. Error bars indicate standard deviation (n=3). (C) Relative expression levels of the indicated mobile elements upon germline-specific knockdown of *armi* and *spn-E* are shown. Depletion of Yb served as control. Fold changes relative to dsRNA against *w* (indicated by red line) were calculated. Measurements were carried out on RNA extracted from whole female flies. Error bars indicate standard deviation (n=3). (D) Scheme of the screen setup. A germline-specific driver, *nos-GAL4*, was used to express UAS-dsRNA constructs in germ cells of the developing oocyte. UAS-*Dcr2* was co-expressed specifically in germ cells to enhance the RNAi response. 2.5 day old female offspring flies were collected and following RNA isolation and reverse transcription probed for de-repression of four transposons by qPCR. Crosses were carried out in trays of 96 that contained a positive (*armi*) and negative (*w*) control knockdown.

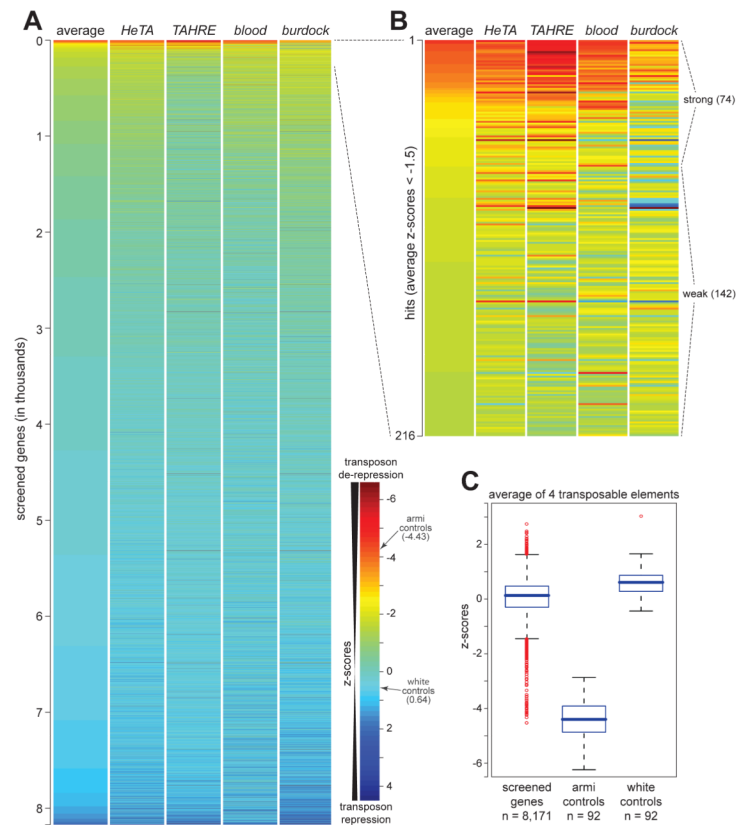


Figure 2. Summary of primary screen and determination of candidate hits

(A) Heat map displaying transposon de-repression (as z-scores) for all 8,171 investigated ovary-expressed genes in red-blue scale. The average of the four tested transposons is shown along the separate z-scores of *HeTA*, *TAHRE*, *blood*, and *burdock*. Negative z-scores indicate transposon de-repression (shown in red). (B) Close-up of the heat map for 216 candidate hits with z-scores < -1.5. (C) Box plots summarizing z-scores of all screened genes, positive *armi* controls, and negative *w* controls. Average data from four transposons was used for the analysis.

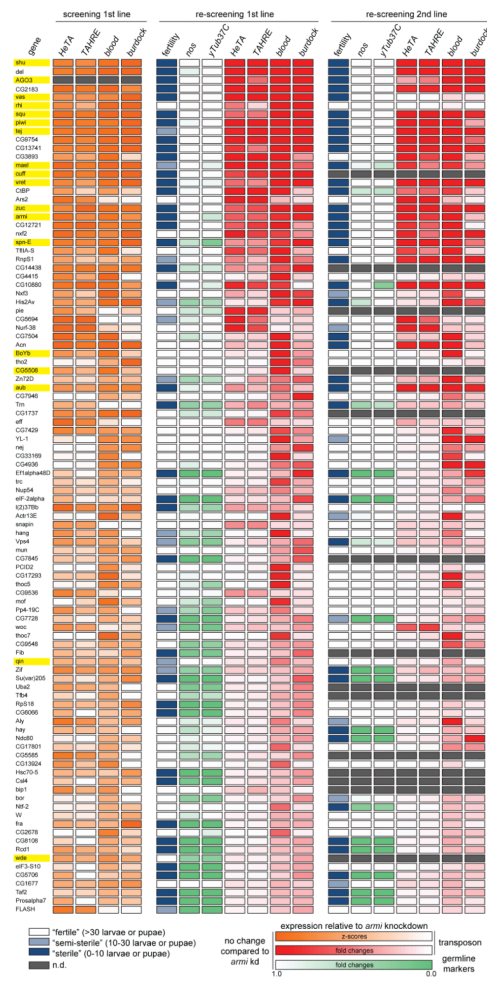


Figure 3. Identification and validation of strong candidate genes
 Heat maps summarizing transposon de-repression, germline marker gene expression, and sterility phenotypes upon germline-specific knockdown of indicated genes. Data is presented relative to depletion of Armi. Yellow boxes highlight known piRNA pathway components.

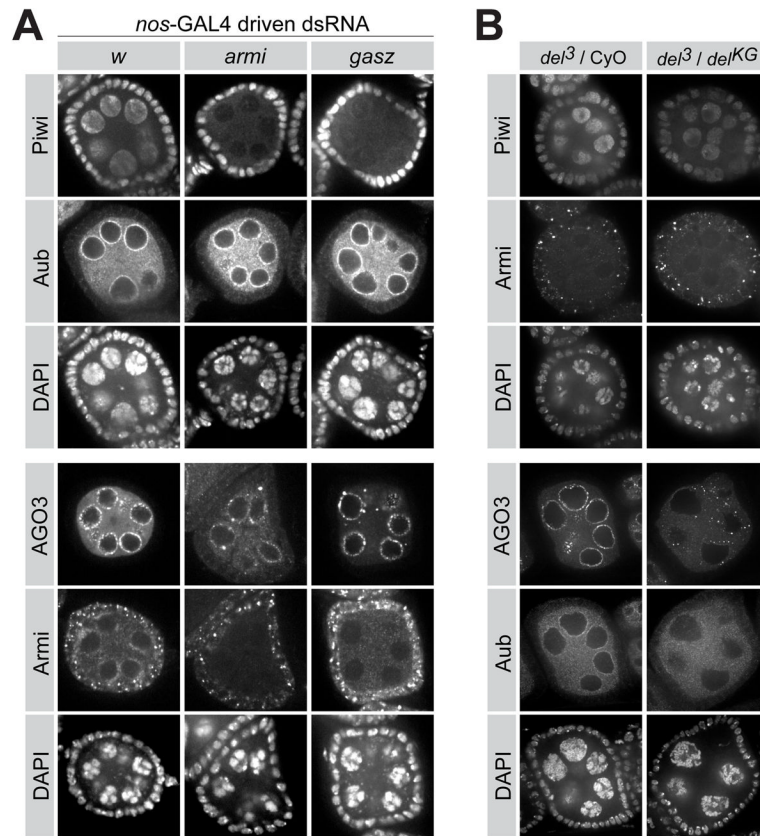


Figure 4. Subcellular localization phenotypes upon depletion of the piRNA pathway candidate factors GASZ and Del

(A) Knockdown of *armi* and *gasz* in the germline using *nos-GAL4* causes Piwi delocalization from nuclei and redistribution of Armi from nuage-like sites. The localization of Aub and AGO3 is not changed. Knockdown of *w* is shown as control. (B) Loss-of-function allelic combination *del³/del^{KG}* severely impairs the localization of secondary piRNA pathway components Aub and Ago3, while Piwi and Armi are unaffected.

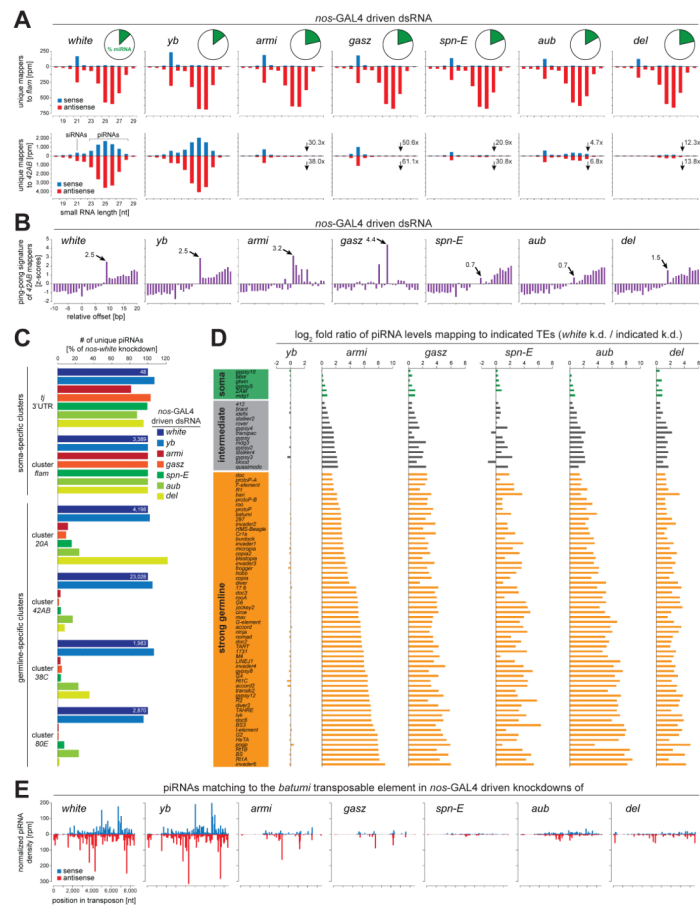


Figure 5. Germline knockdown of *gasz* or *del* affects different steps of piRNA biogenesis
(A) Size distribution of 18- to 29-nt small RNAs derived from each strand of the *flam* and *42AB* clusters are shown as histogram (blue sense; red antisense). The fraction of miRNAs (green) for the indicated libraries is highlighted in the pie charts. **(B)** Histograms showing the relative enrichment of piRNAs overlapping by the indicated number of nucleotides are plotted for *42AB*-derived sequences in the indicated knockdowns. A peak at position 9 (arrow, the number corresponds to the z-score) is suggestive of a ping-pong signature. **(C)** A histogram showing relative piRNA levels of a series of soma- and germline-dominant clusters. Total reads were normalized across libraries to *flam*-unique piRNAs, which are unaffected by *nos*-GAL4-specific knockdowns. Changes in piRNA levels are shown with reference to depletion of *w* (set to 100%). **(D)** Histograms showing the abundance of piRNAs mapping to soma dominant (green), intermediate (grey), or germline dominant (orange) transposons in *w* knockdowns compared to depletion of the indicated genes (log₂ scale). **(E)** Histograms of piRNAs mapping to the consensus sequence of the germline dominant *batumi* LTR transposon, are shown for the indicated knockdowns.

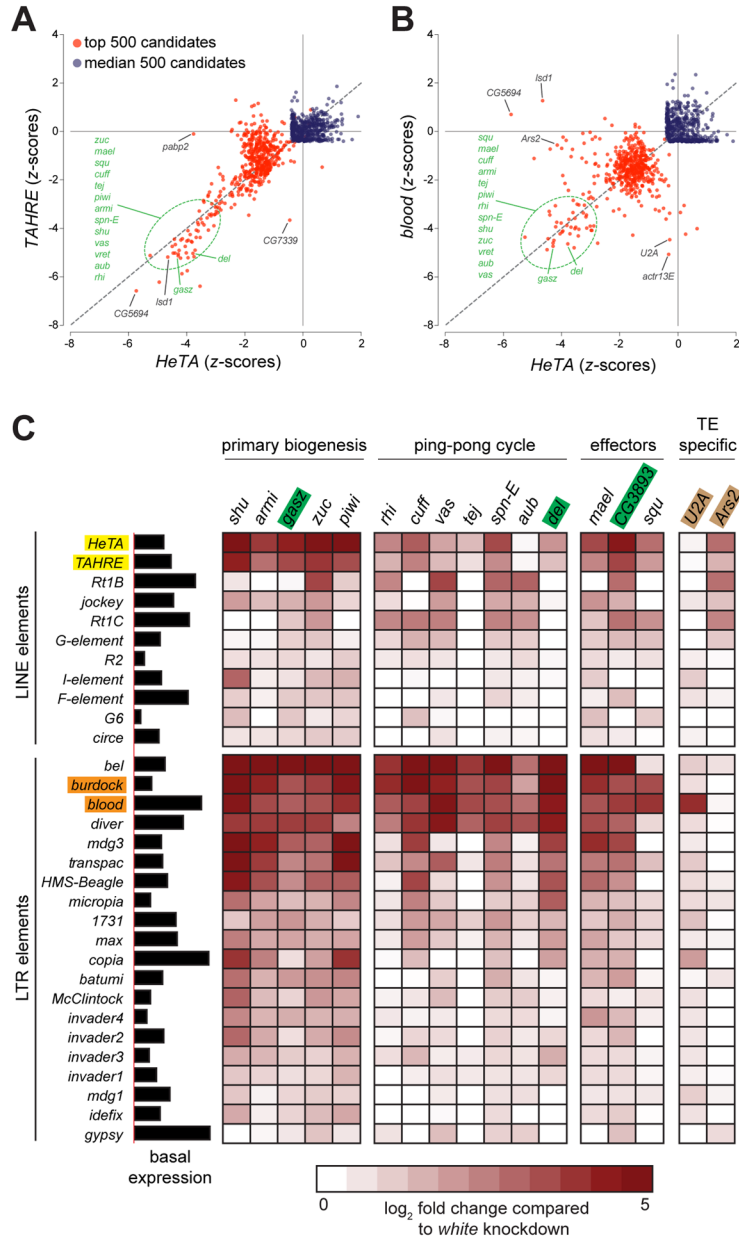


Figure 6. Specific requirements for silencing of different transposon types
(A) Scatter plot comparing transposon de-repression (as z-scores) for *HeTA* and *TAHRE* (top 500 candidates from the primary screen are shown in red, median 500 candidates are indicated in blue). Known piRNA pathway components are highlighted in green. **(B)** Similar as in (A), but *HeTA* de-repression is compared to transposon up-regulation of the LTR element *burdock*. **(C)** Heat map probing transposon de-silencing for known and newly identified piRNA pathway components. *U2A* and *Ars2* represent factors required for silencing of a subset of transposable elements only. Transposon de-silencing is displayed as normalized read count mapping to the canonical sequence for each element relative to a baseline calculated from the average of five independent negative controls (log₂ scale).

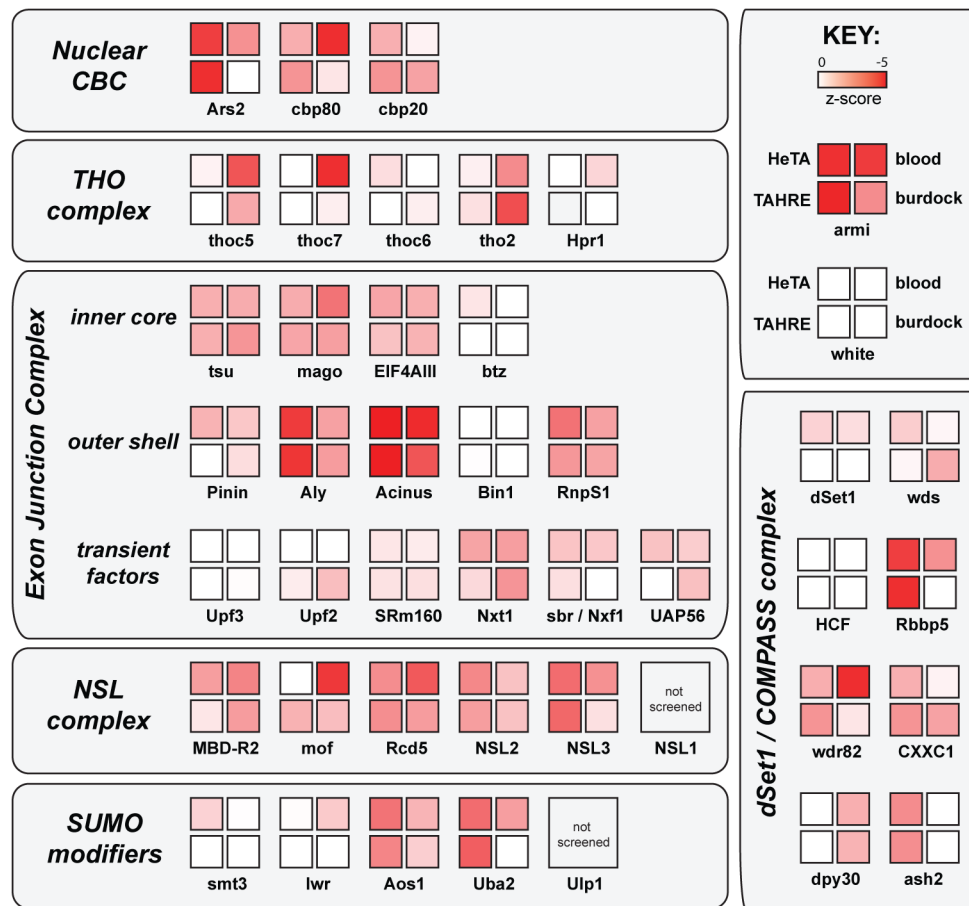


Figure 7. Protein complexes implicated in silencing of germline transposons

Primary screen data is summarized for six known *Drosophila* macromolecular complexes: the nuclear cap binding complex (CBC), the THO complex, the EJC, the NSL complex, components of the SUMOylation machinery, and the H3K4 methyltransferase dSet1/COMPASS complex. Color-coding of boxes indicates the transposon z-scores measured for each gene as exemplified in the key at upper right (for *armi* and *w* knockdowns).